J. Am. Chem. Soc. **1986**, *108*, 8241–8249 8241

(13), 314.20 (43), 299.20 (38), 296.20 (21), 281.15 (16), 271.15 (20), 253.15 (15), 229.15 (13), 213.15 (10), 55.05 (100).

[6-^{3}H]-(25*R*)-24-Methylene-27-methyl-3α,5-cyclocholestan-6α-ol (43a). This compound was obtained from the ketone **42a**: ^{1}H NMR (300 MHz) δ 4.692 (2 H, s, C-28), 1.000 (3 H, d, J = 6.8 Hz, C-25), 0.932 (3 H, d, J = 6.7 Hz, C-21), 0.912 (3 H, s, C-19), 0.828 (3 H, t, J = 7.3 Hz, C-29), 0.684 (3 H, s, C-18); low-resolution mass spectrum, m/z (relative intensity) 412.40 (M$^+$, 4), 397.40 (25), 394.40 (10), 379.40 (12), 357.35 (15), 314.35 (62), 299.50 (54), 296.30 (31), 281.30 (25), 271.30 (33), 253.20 (26), 245.20 (13), 231.15 (14), 225.15 (19), 213.15 (16), 55.15 (100).

[6-^{3}H]-24(28)-Dehydroaplysterol (44a,b). Each labeled 3α,5-cyclocholestan-6α-ol was dissolved in dioxane/water (4:1, 3 mL), containing *p*-toluenesulfonic acid (3 mg), and heated at 90 °C for 4 h. After the mixture cooled to room temperature, sodium carbonate and hexane were added, and the organic layer was then transferred to a short silica gel column and eluted with hexane/ether (5:1) to afford the tritium-labeled [6-^{3}H]-24(28)-dehydroaplysterol, which was further purified by reverse-phase HPLC (mobile phase, methanol). Identity was confirmed by comparison of the NMR spectra of nonradioactive samples (prepared by sodium borohydride reduction) with synthetic sterols. Thus **44** was obtained from **5** in an overall yield of 25%.

Incorporation Experiments. The sponge specimens were collected along the outer reef slope (25 m) near Madang, Papua New Guinea, and transplanted onto plastic plaques at least 1 month prior to use. The precursors were incorporated into duplicate plaques via 11-h aquarium incubations and returned to the sea for 30 days before being collected according to a previously described method.[6] These experiments were performed in two groups with codisterol, epicodisterol, 24(28)-dehydroaplysterol, and 24(28)-dehydroepiaplysterol incorporations initiated on June 7, 1985 and all others initiated on October 19, 1985. Specimens were air-dried at the collecting site before being shipped to California for analysis.

Acknowledgment. Financial support was provided by NIH Grants GM06840 and GM28352 and by the Christensen Fund (U.S.A.). A grant by the Chevron Oil Field Research Company helped defray the cost of radiolabeled reagents. Use of the 300-MHz ^{1}H NMR facility at Stanford was made possible by NSF Grant CHE81-09064. We thank Prof. R. D. Simoni for the use of his liquid scintillation counter, Ruth Records for recording low-resolution mass spectra, the University of California at Berkeley (Bio-organic, Biomedical Mass Spectrometry Resource supported by NIH Grant no. RR 01614) for high-resolution mass spectral determinations, J. Pierret, T. Frohm, and B. Thompson for field assistance, and C. D. Christensen for logistical support. This is Contribution No. 1 from the Christensen Research Institute.

Electronic Structure of Piano-Stool Dimers. 3. Relationships between the Bonding and Reactivity of the Organically Bridged Iron Dimers $[CpFe(CO)]_2(\mu\text{-}CO)(\mu\text{-}L)$ (L = CO, CH_2, $C{=}CH_2$, CH^+)[1]

Bruce E. Bursten*[2] and Roger H. Cayton

Contribution from the Department of Chemistry, The Ohio State University, Columbus, Ohio 43210. *Received June 23, 1986*

Abstract: The electronic structures of the title molecules have been investigated via Fenske–Hall molecular orbital calculations. A fragment analysis is used wherein the $[CpFe(CO)]_2(\mu\text{-}CO)$ dinuclear, singly bridged framework is allowed to interact with CO, CH_2, $C{=}CH_2$, or CH^+ as a second bridging ligand. The changes in electronic structure that result from changing the second bridging ligand correlate very well with the changes in the energies and spatial characteristics of the frontier orbitals of the bridging ligands. The diverse chemistry of these dimers with nucleophiles and electrophiles is shown to correlate with the bridging ligand induced changes in electronic structure. The photochemical reactions of these systems, either in the absence of additional ligands or in the presence of alkynes or phosphines, are shown to be "LUMO-controlled". A scheme is proposed to explain the varied photochemical reactions of $[CpFe(CO)]_2(\mu\text{-}CO)_2$ and its bridge-substituted derivatives.

Hydrocarbyl-bridged transition-metal dimer complexes constitute a class of molecules which has been the focus of much recent research in organometallic chemistry.[3] This interest has been fueled by the prospect of such complexes behaving as models for catalytic surface chemistry. Many transition-metal dimer frameworks have demonstrated the ability to support a variety of organic bridging units, and one structural class that has received particular attention is the $[CpML_n]_2(\mu\text{-}L')_m$ (Cp = η^5-C_5H_5) or "piano-stool dimer" system. These structures can be visualized as two $CpML_n$ "piano-stool" complexes bridged through their "legs". Complexes of this type, where L = CO or NO and L′ = an organic moiety, are known for many transition metals and organic units. The electronic versatility of these dimers (achieved by altering either the transition metal or the number and types of ligands L and L′) has succeeded in making these systems very amenable to synthetic and mechanistic investigations.

Perhaps the most synthetically explored piano-stool dimer complexes are those derived from the iron triad having the general formula $[CpM(CO)_2](\mu\text{-}CO)(\mu\text{-}L')$ where M = Fe or Ru and L′ is an organic, formally two-electron donor fragment. The chemistry of these compounds is rapidly expanding and already includes facile cis/trans isomerization,[4] photolytic insertion of small molecules,[5] protonation,[6] hydride abstraction,[7] oxidatively induced

---

[1] For parts 1 and 2 of this series, see: (a) Blaha, J. P.; Bursten, B. E.; Dewan, J. C.; Frankel, R. B.; Randolph, C. L.; Wilson, B. A.; Wrighton, M. S. *J. Am. Chem. Soc.* **1985**, *107*, 4561–4562. (b) Bursten, B. E.; Cayton, R. H. *Organometallics* **1986**, *5*, 1051–1053.

[2] Camille and Henry Dreyfus Foundation Teacher-Scholar (1984–1989) and Fellow of the Alfred P. Sloan Foundation (1985–1987).

[3] See, for example: Holton, J.; Lappert, M. F.; Pearce, R.; Yarrow, P. I. W. *Chem. Rev.* **1983**, *83*, 135–201, and references therein.

[4] (a) Adams, R. D.; Cotton, F. A. *J. Am. Chem. Soc.* **1973**, *95*, 6589–6594. (b) Kirchner, R. M.; Marks, T. J.; Kristoff, J. S.; Ibers, J. A. *J. Am. Chem. Soc.* **1973**, *95*, 6602–6613.

0002-7863/86/1508-8241$01.50/0

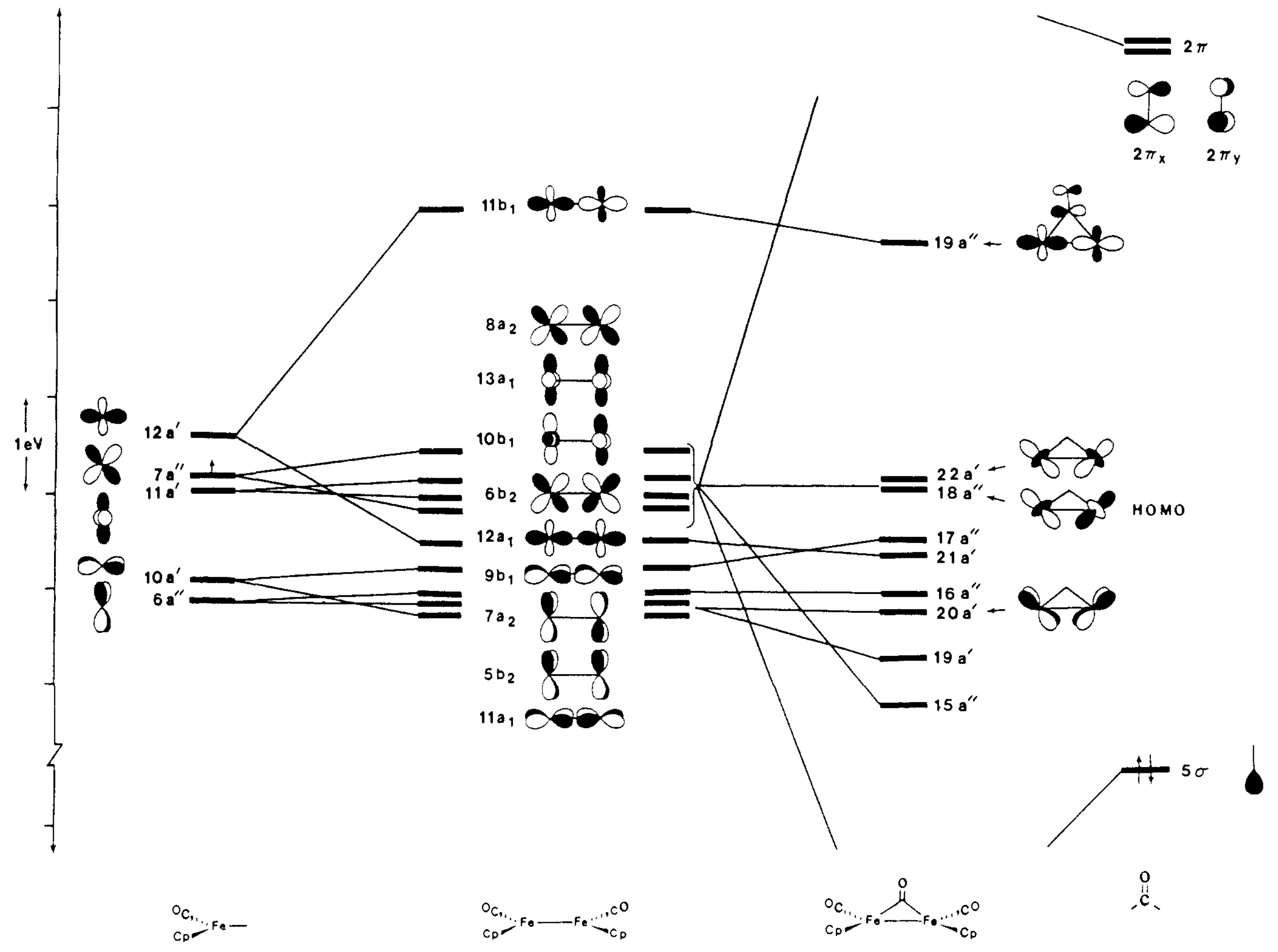

Figure 1. Molecular orbital diagram showing the evolution of the frontier orbitals of the $[(\eta^5\text{-}C_5H_5)Fe(CO)]_2(\mu\text{-}CO)$ framework.

deprotonation,[8] nucleophilic addition,[9] and ylide addition[10] among the reactions possible for the various organic bridges. Despite this seemingly insatiable interest in the synthesis and reactivity of these important systems, theoretical investigations of them have been sparse. Moreover, the theoretical descriptions to date have focused on the spectroscopic properties[11] or geometric preferences[12] of this system rather than their reactivity patterns. Earlier studies in our group have demonstrated the successful application of approximate molecular orbital theory toward the understanding of the acid-base reactivity of half-sandwich or monomeric piano-stool complexes.[13] This contribution represents an extension of this methodology into dimeric piano-stool systems; in particular, we present a theoretical investigation of the piano-stool dimer framework $[CpFe(CO)]_2(\mu\text{-}CO)$ and its interaction with organic bridges such as CO, CH_2, $C{=}CH_2$, CH^+, and CH_3^+. Particular emphasis has been placed upon the correlation of the reactivity of these bridges with their electronic interaction with the dimer framework. It will be demonstrated that, in most cases, the reactivities of these piano-stool dimers are dictated by the electronic demands placed on the framework by the bridging organic ligand.

Computational Details

Molecular orbital calculations were performed on an IBM 3081-D computer system by using the Fenske–Hall nonempirical approximate

---

(5) (a) Dyke, A. F.; Knox, S. A. R.; Naish, P. J.; Taylor, G. E. *J. Chem. Soc., Chem. Commun.* **1980**, 409–410. (b) Dyke, A. F.; Knox, S. A. R.; Naish, P. J.; Taylor, G. E. *J. Chem. Soc., Chem. Commun.* **1980**, 803–805. (c) Casey, C. P.; Miles, W. H.; Fagan, P. J.; Haller, K. J. *Organometallics* **1985**, *4*, 559–563. (d) Hoel, E. L.; Ansell, G. B.; Leta, S. *Organometallics* **1984**, *3*, 1633–1637. (e) Davies, D. L.; Dyke, A. F.; Endsfelder, A.; Knox, S. A. R.; Naish, P. J.; Orpen, A. G.; Plaas, D.; Taylor, G. E. *J. Organomet. Chem.* **1980**, *198*, C43–C49. (f) Adams, P. Q.; Davies, D. L.; Dyke, A. F.; Knox, S. A. R.; Mead, K. A.; Woodward, P. *J. Chem. Soc., Chem. Commun.* **1983**, 222–224. (g) Dyke, A. F.; Knox, S. A. R.; Naish, P. J.; Taylor, G. E. *J. Chem. Soc., Dalton Trans.* **1982**, 1297–1307. (h) Gracey, B. P.; Knox, S. A. R.; Macpherson, K. A.; Orpen, A. G.; Stobart, S. R. *J. Chem. Soc., Dalton Trans.* **1985**, 1935–1944. (i) Dyke, A. F.; Guerchais, J. E.; Knox, S. A. R.; Roue, J.; Short, R. L.; Taylor, G. E.; Woodward, P. *J. Chem. Soc., Chem. Commun.* **1981**, 537. (j) Davidson, J. L.; Green, M.; Stone, F. G. A.; Welch, A. J. *J. Chem. Soc., Dalton Trans.* **1976**, 2044–2053.

(6) (a) Davies, D. L.; Gracey, B. P.; Guerchais, V.; Knox, S. A. R.; Orpen, A. G. *J. Chem. Soc., Chem. Commun.* **1984**, 841–843. (b) Colborn, R. E.; Davies, D. L.; Dyke, A. F.; Endesfelder, A.; Knox, S. A. R.; Orpen, A. G.; Dietrich, P. *J. Chem. Soc., Dalton Trans.* **1983**, 2661–2668. (c) Davies, D. L.; Dyke, A. F.; Endesfelder, A.; Knox, S. A. R.; Naish, P. J.; Orpen, A. G.; Plaas, D.; Taylor, G. E. *J. Organomet. Chem.* **1980**, *198*, C43–C49.

(7) Casey, C. P.; Fagan, P. J.; Miles, W. H. *J. Am. Chem. Soc.* **1982**, *104*, 1134–1136.

(8) Connelly, N. G.; Forrow, N. J.; Gracey, B. P.; Knox, S. A. R.; Orpen, A. G. *J. Chem. Soc., Chem. Commun.* **1985**, 14–17.

(9) (a) Haines, R. J.; DuPreez, A. L. *J. Organomet. Chem.* **1970**, *21*, 181–193. (b) Casey, C. P.; Fagan, P. J. *J. Am. Chem. Soc.* **1982**, *104*, 4950–4951. (c) Casey, C. P.; Fagan, P. J.; Day, V. W. *J. Am. Chem. Soc.* **1982**, *104*, 7360–7361. (d) Casey, C. P.; Marder, S. R.; Fagan, P. J. *J. Am. Chem. Soc.* **1983**, *105*, 7197–7198. (e) Casey, C. P.; Meszaros, M. W.; Marder, S. R.; Fagan, P. J. *J. Am. Chem. Soc.* **1984**, *106*, 3680–3681. (f) Carty, A. J.; Efraty, A.; Ng, T. W.; Birchall, T. *Inorg. Chem.* **1970**, *9*, 1263–1268. (g) Haines, R. J.; DuPreez, A. L. *Inorg. Chem.* **1969**, *8*, 1459–1464. (h) Kao, S. C.; Lu, P. P. Y.; Pettit, R. *Organometallics* **1982**, *1*, 911–914.

(10) (a) Davies, D. L.; Knox, S. A. R.; Mead, K. A.; Morris, M. J.; Woodward, P. *J. Chem. Soc., Dalton Trans.* **1984**, 2293–2299. (b) Korwagen, R.; Alt, R.; Speth, D.; Ziegler, M. L. *Angew. Chem., Int. Ed. Engl.* **1981**, *20*, 1049–1051.

(11) (a) Granozzi, G.; Tondello, E.; Benard, M.; Fragala', I. *J. Organomet. Chem.* **1980**, *194*, 83–89. (b) Mitschler, A.; Rees, B.; Lehmann, M. S. *J. Am. Chem. Soc.* **1978**, *100*, 3390–3397.

(12) Jemmis, E. D.; Pinhas, A. R.; Hoffmann, R. *J. Am. Chem. Soc.* **1980**, *102*, 2576–2585.

(13) (a) Bursten, B. E.; Gatter, M. G. *J. Am. Chem. Soc.* **1984**, *106*, 2554–2558. (b) Bursten, B. E.; Gatter, M. G. *Organometallics* **1984**, *3*, 941–943.

Table I. Bond Lengths, Bond Angles, and Deleted Orbitals for Each of the Fragments Investigated

fragment	bond distances		bond angles		deleted orbitals
$[CpFe(CO)]_2(\mu\text{-}CO)$	Fe–Fe	2.531	Fe–[μ-C]–Fe	82.6	
	Fe–C[*t*-CO]	1.745	Fe–Fe–[μ-C]	48.7	
	Fe–C[μ-CO]	1.917	Fe–Fe–[*t*-C]	100.0	
	Fe–C[Cp]	2.1062	Fe–Fe–Cp[a]	135.5	
	C–O[*t*-CO]	1.153	Cp–Fe–[*t*-CO]	124.5	
	C–O[μ-CO]	1.1805	Fe–C–O[*t*-CO]	180.0	
	C–C	1.39152	Fe–C–O[μ-CO]	138.7	
	C–H	1.08			
μ-CO	Fe–C	1.917	Fe–C–O	138.7	3σ, 6σ
	C–O	1.1805			
$\mu\text{-}CH_2$	Fe–C	1.987	H–C–H	109.47	$2b_2$, $3a_1$
	C–H	1.08			
$\mu\text{-}C{=}CH_2$	Fe–C	1.94	H–C–H	120.0	$4a_1$, $3b_1$, $5a_1$
	C–C	1.34			
	C–H	1.08			
$\mu\text{-}CH^+$	Fe–C	1.917	Fe–C–H	138.7	4σ
	C–H	1.08			

[a] Cp indicates the centroid of the C_5H_5 ring.

MO method.[14] In all calculations the structure of the $[CpFe(CO)]_2(\mu\text{-}CO)$ fragment was taken from the crystal structure of *cis*-$[CpFe(CO)](\mu\text{-}CO)_2$[15] and was idealized to C_s symmetry with local D_{5h} symmetry about the cyclopentadienyl rings. The geometry of this fragment was kept constant for all calculations. The structural parameters for the $[CpFe(CO)]_2(\mu\text{-}CO)$ fragment as well as the various bridging units are given in Table I.

All atomic wave functions were generated by using the method of Bursten, Jensen, and Fenske.[16] Contracted double-ζ representations were used for the Fe 3d AO's and for the C and O 2p AO's. An exponent of 1.16 was used for the hydrogen 1s AO's.[17] The basis functions for Fe were derived for the +1 oxidation state with the 4s and 4p exponents fixed at 2.0 and 1.8, respectively. The calculations were performed by using a fragment analysis which will be detailed in a stepwise manner below. The carbonyl 3σ and 6σ orbitals as well as the first three occupied C_5H_5 orbitals and all virtual orbitals above the e_2'' level were deleted from the basis transformation set of the $[CpFe(CO)]_2(\mu\text{-}CO)$ framework.[18] The orbitals deleted from the bridging fragments are given in Table I.

Results and Discussion

In order to facilitate an understanding of the interactions of the various organic bridges with a *cis*-$[CpFe(CO)]_2(\mu\text{-}CO)$ framework, we must first describe the electronic structure of the dimer framework.[19] In particular, attention will be given to the frontier orbitals of the framework which can interact with the bridges. The evolution of these frontier orbitals is illustrated in Figure 1. The framework is assembled from left to right by first joining the two CpFe(CO) fragments, forming an Fe–Fe bond, and then bridging the Fe atoms symmetrically with one carbonyl ligand. The primarily metal-based orbitals of the 15 electron CpFe(CO) moiety have been discussed elsewhere,[20] and their derivation will not be detailed here. Interaction of two of these fragments produces the nonbridged dimer fragment $[CpFe(CO)]_2$, the frontier orbitals of which are sketched in Figure 1. The most significant Fe–Fe interaction is that between the 12a′ orbitals of the CpFe(CO) fragments, giving rise to the occupied $12a_1$ σ-bonding orbital and unoccupied $11b_1$ antibonding orbital. The Fe–Fe bond formed by this interaction is rather weak as the overlap of the two d_{z^2} orbitals is only 0.037 at the Fe–Fe bond length of 2.531 Å. There are two sets of π and δ interactions, all quite weakly Fe–Fe bonding or antibonding, producing a set of four orbitals above the σ-bonding orbital and four orbitals below it. We can now obtain the desired dimer framework by interaction of $[CpFe(CO)]_2$ with a bridging carbonyl ligand. Coordination of a single carbonyl bridge lowers the symmetry from C_{2v} to C_s, which allows mixing between the a_1 and b_2 orbitals and between those of a_2 and b_1 symmetry. This mixing is particularly evident among the block of four closely spaced orbitals $10b_1$–$8a_2$, resulting in the generation of four π–δ hybrid orbitals as shown below. Two of the four resulting hybrids can interact strongly with the CO 5σ and $2\pi_x$ orbitals, while the other two hybrids, which constitute the HOMO and LUMO of the neutral framework, are directed toward the site of a second bridging ligand. The lowest two metal-based orbitals of the nonbridged dimer ($11a_1$ and $5b_2$) also mix producing two π–δ orbitals of a′ symmetry illustrated below.

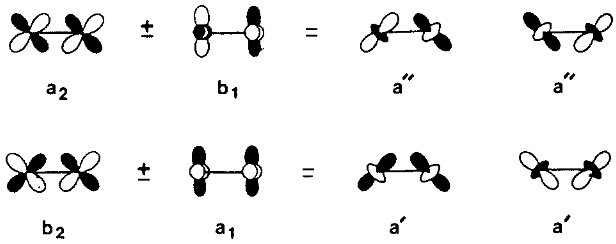

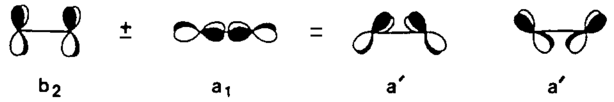

One of these can interact with the CO $2\pi_y$, while the other (the 20a′ orbital) is also directed at the "empty" bridging position. Thus the effect of a bridging CO ligand on the orbitals of $[CpFe(CO)]_2$ is to generate six directed hybrids, three which interact with the CO 5σ and 2π orbitals. The remaining three hybrids (the 20a′, 18a″, and 22a′ orbitals of $[CpFe(CO)]_2(\mu\text{-}CO)$) are directed at the open bridging site. These three orbitals will be the ones principally involved in bonding the bridging organic ligands, and, therefore, we will focus on their interactions from this point on.

Carbonyl and Methylene Bridges

The first bridging ligands we will consider are L′ = CO and L′ = CH_2, which generate the well-known carbonyl- and methylene-bridged complexes $[CpFe(CO)]_2(\mu\text{-}CO)_2$ and $[CpFe(CO)]_2(\mu\text{-}CO)(\mu\text{-}CH_2)$, respectively. Figure 2 depicts the orbital interaction diagrams for these two bridging units with the iron dimer framework. The left half of Figure 2 illustrates the carbonyl

---

[14] Hall, M. B.; Fenske, R. F. *Inorg. Chem.* **1972**, *11*, 768–775.

[15] Bryan, R. F.; Greene, P. T.; Newlands, M. J.; Field, D. S. *J. Chem. Soc. A* **1970**, 3068–3074.

[16] Bursten, B. E.; Jensen, J. R.; Fenske, R. F. *J. Chem. Phys.* **1978**, *68*, 3320–3321.

[17] Hehre, W. J.; Stewart, R. F.; Pople, J. A. *J. Chem. Phys.* **1969**, *51*, 2657–2664.

[18] Lichtenberger, D. L.; Fenske, R. F. *J. Chem. Phys.* **1976**, *64*, 4247–4264.

[19] Calculations on the trans isomer show it to very similar electronically to the cis isomer (see ref 12).

[20] Hofmann, P. *Angew. Chem.* **1979**, *91*, 591–593; *Angew. Chem., Int. Ed. Engl.* **1979**, *18*, 554.

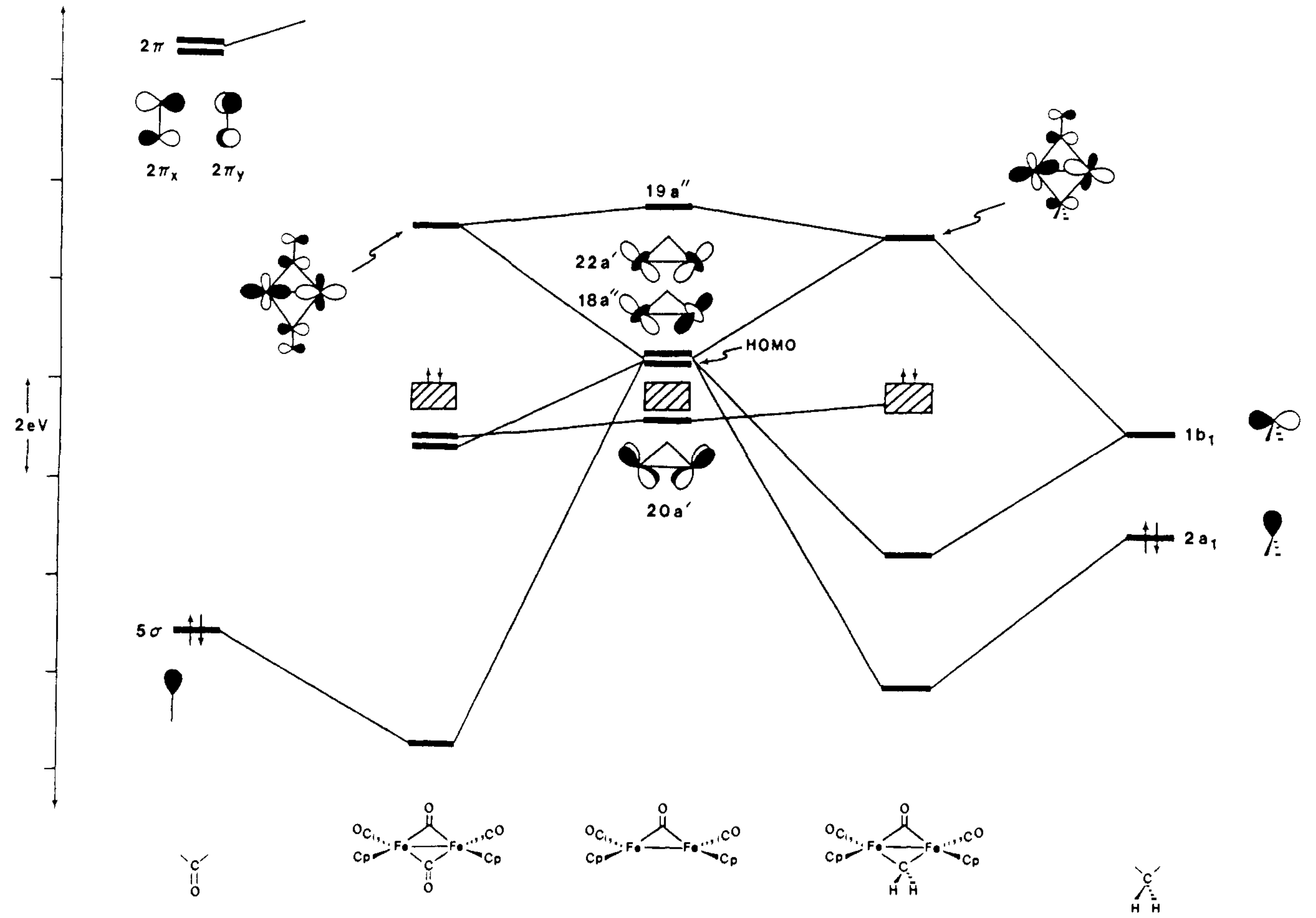

Figure 2. Molecular orbital diagrams of *cis*-$[(\eta^5\text{-}C_5H_5)Fe(CO)]_2(\mu\text{-}CO)_2$ and *cis*-$[(\eta^5\text{-}C_5H_5)Fe(CO)]_2(\mu\text{-}CO)(\mu\text{-}CH_2)$.

interactions. The nearly degenerate set of hybrid orbitals on the $[CpFe(CO)]_2(\mu\text{-}CO)$ framework, constituting the HOMO and LUMO, interact strongly with the CO 5σ and $2\pi_x$ orbitals as the symmetry now returns to C_{2v}. The other framework hybrid, 20a′, forms a weaker interaction with the CO $2\pi_y$. The HOMO of the resulting bis(μ-CO) dimer is in this case a π* orbital similar to the $9b_1$ orbital of $[CpFe(CO)]_2$. The LUMO is Fe–Fe σ* antibonding and Fe-(μ-CO) antibonding and is essentially a symmetrized analogue of orbital 19a″ of the dimer framework.

Previous calculations of varying rigor have been performed on $[CpFe(CO)]_2(\mu\text{-}CO)_2$ and agree in a qualitative sense with those presented here.[11,12,21] With the exception of the ab initio work of Benard,[21] it is generally agreed that the LUMO is an energetically isolated, primarily Fe–Fe σ* orbital (similar to that pictured in Figure 2). The nature of the HOMO, however, tends to be more method-dependent which is not unexpected since the orbitals of Fe–Fe character just beneath the HOMO are very closely spaced in energy. The Fenske–Hall results reported here, in agreement with the earlier calculations, support the lack of any strong, direct Fe–Fe interaction and favor a delocalized picture of the bonding through the carbonyl bridges. This has also been substantiated experimentally via low-temperature electron density studies.[11b]

The position of the only substantial Fe–Fe interaction (σ-bond) can also be probed experimentally. Theoretical studies by Sherwood and Hall on the electronically similar $Cp_2Fe_2[Ph_2P(CH_2)_nPPh_2](\mu\text{-}CO)_2{}^{0/+1}$ ($n = 0, 1$) show that the Fe–Fe bond length changes little upon oxidation thus providing evidence that the HOMO is not the Fe–Fe σ bond but rather a weaker interaction.[22] Wrighton et al. assign the 346-nm absorption in the UV–vis spectrum of $[CpFe(CO)]_2(\mu\text{-}CO)_2$ at room temperature and 77 K to the $\sigma \rightarrow \sigma^*$ excitation.[23] At lower energy other absorptions are also present (410 nm, 514 nm) indicating that the $\sigma \rightarrow \sigma^*$ excitation is not the lowest energy one possible. Our calculations agree with these experimental observations since our calculated HOMO is π* (perpendicular to μ-CO bridges) in character, and the Fe–Fe σ bond lies below it. Further, the energetic separation between the Fe–Fe σ and σ* orbitals is calculated to be 3.48 eV (28 070 cm^{-1}) which is close to the value of the $\sigma \rightarrow \sigma^*$ excitation (28 902 cm^{-1}) measured by Wrighton et al. This agreement is, of course, qualitative, since we have not considered solvent effects or orbital relaxation upon excitation from the $\sigma^2\sigma^{*0}$ to the $\sigma^1\sigma^{*1}$ configuration. The He(I) and He(II) photoelectron spectra of $[CpFe(CO)]_2(\mu\text{-}CO)_2$[11a] further substantiate the Fenske–Hall ordering of the molecular orbitals. Particularly interesting is the sharpness of the lowest ionization energy band, a feature which we would expect due to the essentially nonbonding nature of the HOMO we find. These qualitative correlations of the theoretical description to the experimental results provide an added assurance that the Fenske–Hall molecular orbital treatment produces a sound electronic picture for this system.

The right half of Figure 2 illustrates the molecular orbital diagram which results from allowing a CH_2 ligand to bridge the $[CpFe(CO)]_2(\mu\text{-}CO)$ framework. As must be expected, the major differences between $[CpFe(CO)]_2(\mu\text{-}CO)_2$ and $[CpFe(CO)]_2(\mu\text{-}CO)(\mu\text{-}CH_2)$ result from the differences in the frontier orbitals of CO and CH_2. Singlet methylene has an occupied "σ lone pair" orbital (the $2a_1$) that is spatially similar but energetically somewhat higher than the 5σ orbital of CO, an effect which should make CH_2 a more effective σ donor than CO. A much greater difference

---

(21) (a) Benard, M. *J. Am. Chem. Soc.* **1978**, *100*, 7740–7742. (b) Benard, M. *Inorg. Chem.* **1979**, *18*, 2782–2785.

(22) Sherwood, D. E., Jr.; Hall, M. B. *Inorg. Chem.* **1978**, *17*, 3397–3401.

(23) Abrahamson, H. B.; Palazzotto, M. C.; Reichel, C. L.; Wrighton, M. S. *J. Am. Chem. Soc.* **1979**, *101*, 4123–4127.

is seen in the π orbitals of the two ligands. Whereas CO has a doubly degenerate set of virtual π orbitals, which are quite high in energy, methylene has only one empty π orbital, which is oriented parallel to the Fe–Fe bond. This orbital is much lower in energy than the CO 2π orbitals and is completely localized on the carbon atom, thus facilitating a much stronger interaction with the framework orbitals than was found for CO.

As can be seen in Figure 2, the interactions of the CH_2 $2a_1$ and $1b_1$ orbitals with the dinuclear framework are indeed stronger than the corresponding ones when L′ = CO. The stronger interactions produce several notable electronic differences between the carbonyl- and methylene-bridged dimers. First, more electron density is transferred to the Fe atoms from the filled CH_2 $2a_1$ than from the CO 5σ orbital as is evident in their Mulliken populations (CH_2 $2a_1$ = 1.280 vs. CO 5σ = 1.358). Second and more important, the methylene moiety acts as a better π-acceptor than the carbonyl. The empty CH_2 $1b_1$ orbital is a more effective backbonding orbital and accepts more electron density from the framework than the CO $2\pi_x$ and $2\pi_y$ orbitals combined. This effect is also reflected in the Mulliken populations (CH_2 $1b_1$ = 1.114 vs. CO $2\pi_x + 2\pi_y$ = 0.859). Although the methylene bridge is a better σ donor than carbonyl, its π-acceptor ability dominates, and the overall effect is a more negative charge on the methylene carbon (–0.518) than on the carbonyl carbon (–0.002). The difference in the frontier orbitals of CH_2 and CO also manifests itself in the virtual orbitals of the complex, and we find that the LUMO of the methylene-bridged dimer has a significantly greater contribution from the CH_2 $1b_1$ than from the CO $2\pi_x$. In addition, the lowering of symmetry upon bridging two different ligands induces a mixing of the metal AO's which contribute to the σ^* LUMO such that they are hybridized toward the CO bridge. The result of this "orbital tipping" is to generate an orbital which is now more strongly Fe–CH_2 antibonding while concurrently weakening the Fe–CO antibonding interaction as illustrated below.

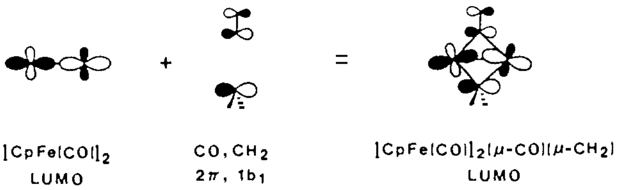

Previous calculations performed on the methylene-bridged piano stool dimers $[CpMn(CO)_2]_2(\mu\text{-}CH_2)$[24] and $[CpRh(CO)]_2(\mu\text{-}CH_2)$[20] have led to the conclusion that these compounds can be considered dimetallacyclopropanes due to their electronic similarity with cyclopropane. These complexes unambiguously possess direct metal-metal bonds, a consequence in part of containing only a single bridging ligand. The absence of a strong Fe–Fe interaction in $[CpFe(CO)]_2(\mu\text{-}CO)(\mu\text{-}CH_2)$ makes it tempting to refer to it as a "2,4-dimetallocyclobutanone". While such a classification is useful only in a formalistic sense, it is useful in pointing out that the reactivity of methylene-bridged complexes containing additional bridges might be different than those without additional bridging ligands. The reactions observed for $[CpFe(CO)]_2(\mu\text{-}CO)(\mu\text{-}L)$ (L = CO, CH_2) will be the focus of the next section.

Reactions of the Carbonyl- and Methylene-Bridged Complexes

The first methylene-bridged dimers which were synthesized exhibited great thermal stability, generally greater than their carbonyl analogues. Thus, it was first thought that the methylene bridge was so robust that the complexes were, somewhat disappointingly, unreactive.[25] Since then, however, a number of interesting reactions have been shown to occur at the bridging group. In this section, we will compare some of the reactions of $[CpFe(CO)]_2(\mu\text{-}CO)_2$ and $[CpFe(CO)]_2(\mu\text{-}CO)(\mu\text{-}CH_2)$ in light of their electronic structural similarities and differences. It is not our intention to provide an exhaustive survey of the reactions of these widely studied compounds. Rather, we will focus on two very different representative reactions, protonation and photochemical alkyne insertion, which we believe are closely tied to electronic structure.

Protonation Reactions. The reaction of dimeric organometallic complexes with H^+ provides an excellent probe of whether electrophilic addition occurs via charge or orbital control. The treatment of $[CpFe(CO)]_2(\mu\text{-}CO)_2$ with HBF_4 in CH_2Cl_2 results in protonation of the complex to yield $[CpFe(CO)_2]_2(\mu\text{-}H)^+$, the proposed structure of which is a symmetrically bridged dimer (eq 1).[26] The initial addition of H^+, if charge-controlled, would occur at the bridging carbonyl since it is the most negatively charged site in the molecule (q_C = –0.12; q_O = –0.15). We propose, however, that this is an orbital-controlled reaction in which the electrophile H^+ seeks out the highest occupied orbitals of the complex. Our calculations indicate that the HOMO of the complex is a weakly π antibonding orbital to which the proton could not add symmetrically. The second highest occupied MO (SHOMO) of the complex, only 0.30 eV below the HOMO, is the weak σ bond of the complex to which the proton could add symmetrically. Thus, proton attack of the HOMO would lead to an asymmetric protonated dimer that could then rearrange to the symmetric μ-H complex, which may be viewed formally as a donor–acceptor complex formed from $CpFe(CO)_2H$ and $CpFe(CO)_2^+$. The proton could also attack the SHOMO of the complex, leading directly to the symmetrically bridged dimer. In either case, it seems likely that the Fe–H–Fe linkage would resemble that of $[Cr(CO)_5]_2(\mu\text{-}H)^-$ in which a three-center, two-electron bond has been proposed.[27]

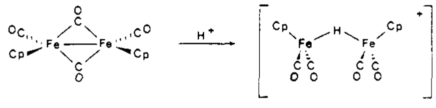

(1)

The treatment of $[CpFe(CO)]_2(\mu\text{-}CO)(\mu\text{-}CH_2)$ with H^+ leads to very different chemistry. Although the uppermost occupied MO's of the methylene-bridged complex strongly resemble those of $[CpFe(CO)]_2(\mu\text{-}CO)_2$, there is no evidence for addition of H^+ to the Fe–Fe bond. Rather, the complex is protonated at the methylene to yield a methyl-bridged dimer which contains an agostic C–H bond (eq 2).[7] A description of the electronic structure, bonding, and geometric preference of the methyl-bridged complex has been presented in a separate contribution.[1b] Why is the product of H^+ addition so different for the methylene-bridged complex? There are two primary reasons. First, if the proton added symmetrically to the Fe–Fe bond, the greatly increased Fe–Fe distance would force the methylene ligand to adopt a terminal conformation. CO ligands have no difficulty interconverting between bridged and terminal bonding, but we know of only a few such conversions (generally in rather unusual complexes) for alkylidene ligands.[28] Second, and perhaps more important, the replacement of a μ-CO by a μ-CH_2 results in a much more negatively charged carbon bridge. Our calculated Mulliken charges for the μ-C in $[CpFe(CO)]_2(\mu\text{-}CO)_2$ and the μ-(CH_2) in $[CpFe(CO)]_2(\mu\text{-}CO)(\mu\text{-}CH_2)$ are –0.12 and –0.52, respectively. Thus we believe that upon replacement of μ-CO by μ-CH_2, proton addition switches from orbital to charge control.

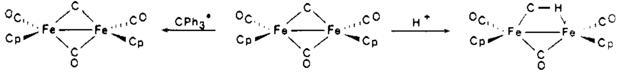

(2)

Further evidence for the above view is provided by the reactions of $[CpFe(CO)]_2(\mu\text{-}CO)(\mu\text{-}CH_2)$ with bulky electrophiles which

---

(24) Calabro, D. C.; Lichtenberger, D. L.; Herrmann, W. A. *J. Am. Chem. Soc.* **1981**, *103*, 6852–6855.

(25) Herrmann, W. A. *Adv. Organomet. Chem.* **1982**, *20*, 159–263, and references therein.

(26) Legzdins, P.; Martin, D. T.; Nurse, C. R.; Wassink, B. *Organometallics* **1983**, *2*, 1238–1244.

(27) Eyermann, C. J.; Chung-Phillips, A. *Inorg. Chem.* **1984**, *23*, 2025–2029.

(28) (a) Herrmann, W. A.; Bauer, C. *Organometallics* **1982**, *1*, 1101–1102. (b) Messerle, L.; Curtis, M. D. *J. Am. Chem. Soc.* **1982**, *104*, 889–891.

Scheme I. Three Possible Pathways for the Photochemical Insertion of Alkynes into One of the Fe–(μ-CO) Bonds of $[(\eta^5\text{-}C_5H_5)Fe(CO)]_2(\mu\text{-}CO)_2$

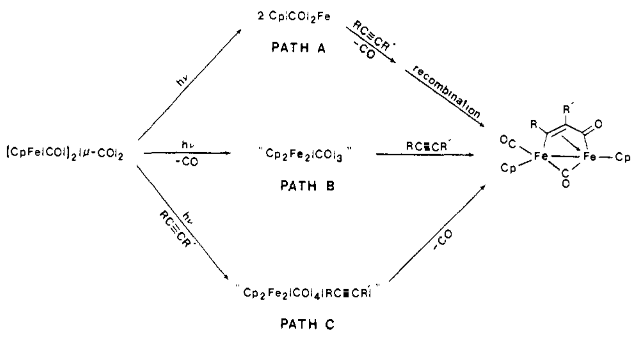

are incapable of adding to the μ-CH_2. As an example, the treatment of the complex with the trityl cation (CPh_3^+) leads to the formation of the methylidyne-bridged cation (eq 2).[7] While this may be viewed as a simple hydride-abstraction reaction, it is believed that trityl acts as a one-electron oxidizing agent forming first the radical cation $[CpFe(CO)]_2(\mu\text{-}CO)(\mu\text{-}CH_2)^{\bullet+}$, which then loses hydrogen producing the methylidyne-bridged cation.[29] Cleavage of the Fe–Fe bond does not occur, an observation consistent with the weakly π-antibonding nature of the HOMO of $[CpFe(CO)]_2(\mu\text{-}CO)(\mu\text{-}CH_2)$. Later on in this paper we will discuss the electronic structure of $[CpFe(CO)]_2(\mu\text{-}CO)(\mu\text{-}CH)^+$ and examine the electronic motivation for its formation.

Photochemical Alkyne Insertion. An interesting reaction which occurs for both $[CpFe(CO)]_2(\mu\text{-}CO)_2$ and $[CpFe(CO)]_2(\mu\text{-}CO)(\mu\text{-}CHR)$ is the photochemical insertion of alkynes into one of the Fe-(μ-C) bonds (eq 3 and 4).[5a,b] In each case this results in the expulsion of one CO and the formation of an unsaturated five-membered metallacycle in which the double bond is coordinated to one of the Fe atoms. As there is very little known about the electronic basis or mechanisms for these reactions, we will examine them here in light of our calculations.

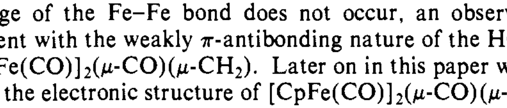

(3)

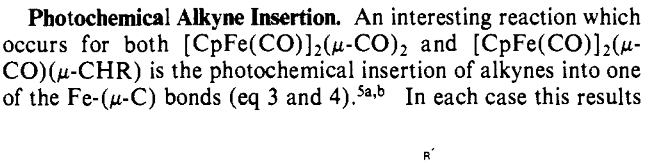

(4)

$[CpFe(CO)]_2(\mu\text{-}CO)_2$ exhibits a rich photochemistry in the absence of additional ligands. Wrighton and co-workers have provided convincing evidence that $Cp(CO)_2Fe^\bullet$ radicals are generated upon broadband irradiation of $[CpFe(CO)]_2(\mu\text{-}CO)_2$;[23] however, more recently it has been shown that irradiation of $[(\eta^5\text{-}C_5R_5)Fe(CO)]_2(\mu\text{-}CO)_2$ (R = H, Me) can also cause CO loss without cleavage, yielding the paramagnetic triply-bridged dimer $[(\eta^5\text{-}C_5R_5)Fe]_2(\mu\text{-}CO)_3$.[1a,30,31] Experiments performed by Caspar and Meyer, by using laser flash photolysis at $\lambda > 250$ nm and $\lambda > 400$ nm, agree with those of Wrighton et al. Two intermediates were detected: a short-lived intermediate thought to be the monomeric cleavage product and a long-lived intermediate which was assigned as being the CO loss product.[32] Turner, Poliakoff, et al. have very recently shown that the broadband photolysis of $[(\eta^5\text{-}C_5Me_5)Fe(CO)]_2(\mu\text{-}CO)_2$ in cyclohexane solution leads to the formation of both mononuclear radicals and the CO loss product within 10 μs of irradiation.[33]

Scheme II. Proposed Transition State and Intermediates in the Photolysis of $[(\eta^5\text{-}C_5H_5)Fe(CO)]_2(\mu\text{-}CO)_2$ and Their Decay Products in the Absence and Presence of an Alkyne Ligand

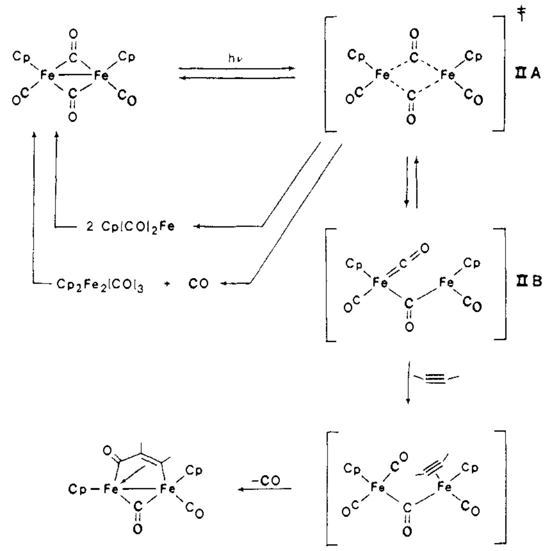

The photolysis of $[CpFe(CO)]_2(\mu\text{-}CO)_2$ in the presence of a two-electron ligand L can yield the dinuclear substitution product $Cp_2Fe_2(CO)_3L$, again without apparent cleavage of the dimer to monomers.[34]

It seems evident from the above that the photochemical reaction of $[CpFe(CO)]_2(\mu\text{-}CO)_2$ with RC≡CR could proceed by three general pathways as shown in Scheme I. In Path A, the Fe–Fe bond is cleaved to monomer fragments which then react with the alkyne and dimerize with CO loss to form the product. Path B involves initial CO dissociation, generating a coordinatively and electronically unsaturated intermediate, followed by alkyne addition to form the dimetallacycle. Path C postulates the initial addition of RC≡CR followed by CO expulsion upon dimetallacycle formation and as such represents an associative addition of RC≡CR. Tyler, Schmidt, and Gray have provided convincing experimental evidence that an associative mechanism is responsible for the photosubstitution of CO by phosphine and phosphite ligands.[34]

Path A seems unlikely based upon the photochemical alkyne insertion experiment performed by Knox et al. wherein the heterobimetallic compound $[Cp_2FeRu(CO)_2](\mu\text{-}CO)_2$ was used in place of $[CpFe(CO)]_2(\mu\text{-}CO)_2$. The only insertion product obtained from this reaction was the mixed-metal Fe–Ru complex.[5h] Between the remaining two paths, both of which preserve the integrity of the dinuclear unit, our calculations lend strong support to the initial step of the associative mechanism shown in path C. The LUMO of $[CpFe(CO)]_2(\mu\text{-}CO)_2$ is Fe–Fe and Fe–(μ-C) antibonding, and it is energetically isolated by >2 eV from higher lying virtual orbitals. Thus, we expect the photochemistry of the complex to be dominated by the excitation of an electron into the LUMO, and such excitation should weaken both the Fe–Fe and Fe–(μ-CO) bonds. However, as was discussed earlier, the Fe–Fe interaction is very weak in the ground state, and we believe that the carbonyl bridges are principally responsible for the integrity of the dimer. Therefore, based upon this electronic description, we propose the pathway shown in Scheme II for the photochemical insertion of alkynes.

Initial photolysis produces the transition state IIA where the Fe–Fe interaction has been eliminated and the Fe–(μ-C) bonds significantly weakened due to the strain of the distorted four-membered ring. The observed photochemistry of $[CpFe(CO)]_2(\mu\text{-}CO)_2$ is consistent with four competitive pathways for

---

(29) Casey, C. P., personal communication.

(30) Hepp, A. F.; Blaha, J. P.; Lewis, C.; Wrighton, M. S. *Organometallics* **1984**, *3*, 174.

(31) Hooker, R. H.; Rest, A. J. *J. Chem. Soc., Chem. Commun.* **1983**, 1022.

(32) Caspar, J. V.; Meyer, T. J. *J. Am. Chem. Soc.* **1980**, *102*, 7794–7795.

(33) (a) Moore, B. D.; Poliakoff, M.; Turner, J. J. *J. Am. Chem. Soc.* **1986**, *108*, 1819–1822. (b) Dixon, A. J.; Healy, M. A.; Poliakoff, M.; Turner, J. T. *J. Chem. Soc., Chem. Commun.* **1986**, 994–996.

(34) Tyler, D. R.; Schmidt, M. A.; Gray, H. B. *J. Am. Chem. Soc.* **1983**, *105*, 6018–6021.

the relaxation of transition state IIA: it can reform the Fe–Fe and Fe–(μ-C) bonds in the reverse reaction of the proposed photochemical step, fall apart into monomeric radicals, lose CO, or break one of the Fe–(μ-C) bonds to form the 18e/16e intermediate IIB. Intermediate IIB is identical with that proposed by Tyler, Schmidt, and Gray in the photosubstitution of CO by phosphine and phosphite ligands,[34] and we propose that the reaction with alkynes occurs in a similar manner. Coordination of the alkyne to the electron deficient metal of IIB followed by insertion of the alkyne and CO expulsion would lead to the final product. We believe that the motivation for CO expulsion is steric as well as electronic; consistent with this, the thermal reaction of the less sterically hindered piano-stool dimer $[CpRh(CO)]_2(\mu\text{-}CO)$ with alkynes leads to a similar dimetallacycle but without CO loss and without double-bond coordination.[35] It is evident from the above discussion that we expect the photochemistry of $[CpFe(CO)]_2(\mu\text{-}CO)_2$ to be dependent on the wavelength of excitation. Unfortunately, the wavelength dependence of the photochemistry has not been studied; to our knowledge, all prior alkyne insertion experiments have used broadband UV and/or visible excitation. Clearly more experimental studies of the mechanistic aspects of $[CpFe(CO)]_2(\mu\text{-}CO)_2$ photochemistry are necessary to validate these proposals, and we are initiating these in our laboratory.

A crucial assumption in the above discussion is that the photochemistry is induced primarily by exciting an electron into the LUMO of $[CpFe(CO)]_2(\mu\text{-}CO)_2$. We believe that the photochemical reaction of $[CpFe(CO)]_2(\mu\text{-}CO)(\mu\text{-}CH_2)$ with alkynes provides excellent support for this assertion. As discussed above, when one CO is replaced with a CH_2 ligand, the LUMO contains significantly more Fe–(μ-CH_2) than Fe–(μ-CO) antibonding interaction. Thus, excitation into the LUMO of $[CpFe(CO)]_2(\mu\text{-}CO)(\mu\text{-}CH_2)$ would be expected to weaken the Fe–(μ-CH_2) bond more than the Fe–(μ-CO) bond. This is entirely consistent with the observed photochemistry: alkynes insert exclusively into the Fe–(μ-CH_2) bond, leading to an analogue of the alkyne insertion product for $[CpFe(CO)]_2(\mu\text{-}CO)_2$ (eq 4).[5a,b] Further support for LUMO control of photochemical insertion will be presented below in conjunction with the chemistry of the vinylidene-bridged dimer.

Vinylidene and Methylidyne Bridges

The methylene bridge examined above is unable to interact with the framework orbitals which are of π-symmetry and oriented perpendicular to the Fe–(μ-C)–Fe plane; continuing the analogy to cyclopropane or cyclobutanone, the methylene carbon is saturated. In this section we will discuss the effects of introducing unsaturation into the bridging hydrocarbyl ligand by examining the well-known vinylidene- and methylidyne-bridged dimers $[CpFe(CO)]_2(\mu\text{-}CO)(\mu\text{-}C{=}CH_2)$ and $[CpFe(CO)]_2(\mu\text{-}CO)(\mu\text{-}CH)^+$. Although both of these hydrocarbon moieties possess a π-system oriented perpendicular to the Fe–Fe bond, it will be seen that their interactions with the dimer framework are quite different.

Let us begin by examining the frontier orbitals of the vinylidene and methylidyne fragments.[36] These are pictured in Figure 3 along with the frontier orbitals of the methylene moiety for comparison. Like the methylene fragment, the HOMO's of the vinylidene and methylidyne fragments ($3a_1$ and 2σ respectively) are σ-type orbitals similar in orientation and energy to the methylene $2a_1$ orbital. Likewise, the vinylidene $2b_1$ and methylidyne $1\pi_x$ orbitals are empty π-type orbitals analogous to the empty methylene $1b_1$ orbital. Now, however, the unsaturated vinylidene and methylidyne fragments each contain a second π-type frontier orbital (the occupied $1b_2$ and empty $1\pi_y$, respectively) which does not correlate to any of the methylene frontier orbitals. We will see how these additional π-type interactions are responsible for reactivity of the vinylidene and methylidyne bridges not observed with the methylene bridge.

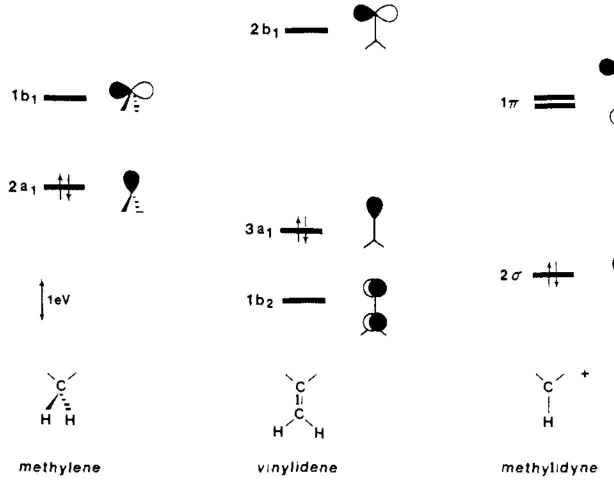

Figure 3. The frontier orbitals of CH_2, $C{=}CH_2$, and CH^+.

Figure 4 contains the molecular orbital diagrams for the interaction of these two unsaturated organic fragments with the iron dimer framework. Considering first the vinylidene case on the left half of the figure, we can see the strong interactions of the $3a_1$ and $2b_1$ vinylidene orbitals with 22a′ and 18a″ of the dimer framework. These interactions are similar to those observed for carbonyl and methylene; therefore, it is not surprising that the vinylidene undergoes similar photolytic insertion reactions. Somewhat surprisingly, the C–C π bond ($1b_2$) scarcely interacts with the dimer framework, largely because this orbital is delocalized on both vinylidene carbon atoms, with a greater contribution from the β carbon. Therefore, the perpendicular π system remains localized on the vinylidene α and β carbons, and the integrity of the C–C π bond is relatively unaffected by coordination to the framework. We will see below how this is consistent with its reactivity. Looking now at the methylidyne ligand on the right half of Figure 3, we can see that the CH^+ 2σ and $1\pi_x$ orbitals, located at the same relative energies as the CH_2 $2a_1$ and $1b_1$ orbitals, interact with 22a′ and 18a″ of the dimer framework in a fashion similar to that of methylene (see Figure 2). However the CH^+ unit has a second empty π orbital, the $1\pi_y$, which is degenerate with the $1\pi_x$. Being at low energy and completely localized on the μ-C, the $1\pi_y$ is able to interact significantly with the framework 20a′ orbital. The result of this additional π interaction is a change in the nature of the LUMO, as compared to the organically bridged dimers presented earlier. The LUMO of the methylidyne-bridged dimer is the antibonding counterpart of the $1\pi_y$–20a′ interaction, and is localized 50% on the methylidyne carbon. It is this orbital which is responsible for some of the very interesting reactivity of this complex.

Reactions of the Vinylidene- and Methylidyne-Bridged Complexes

Reactions at the Vinylidene Bridge. Alkynes have been shown to photochemically insert into the vinylidene-bridged dimer in a fashion similar to that seen earlier for the carbonyl and methylene bridges; in the case of the vinylidene bridge, however, two products were isolated (eq 5).[5c] The second product (resulting from prolonged photolysis) is analogous to alkyne insertion into the methylene bridge in that insertion has occurred in the hydrocarbyl bridge rather than the carbonyl bridge. The isolation of the intermediate product, 5B, which is the result of addition of the alkyne to the vinylidene complex without ligand loss, may provide tenuous support for the proposed associative mechanism. It is not clear that an analogous product is formed in the alkyne addition reactions of the carbonyl- or methylene-bridged dimers,

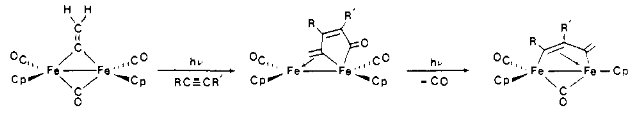

5A **5B** **5C** (5)

---

(35) Dickson, R. S.; Gatehouse, B. M.; Nesbit, M. C.; Pain, G. N. *J. Organomet. Chem.* **1977**, *215*, 97–109.

(36) Kostic, N. M.; Fenske, R. F. *Organometallics* **1982**, *1*, 974–982.

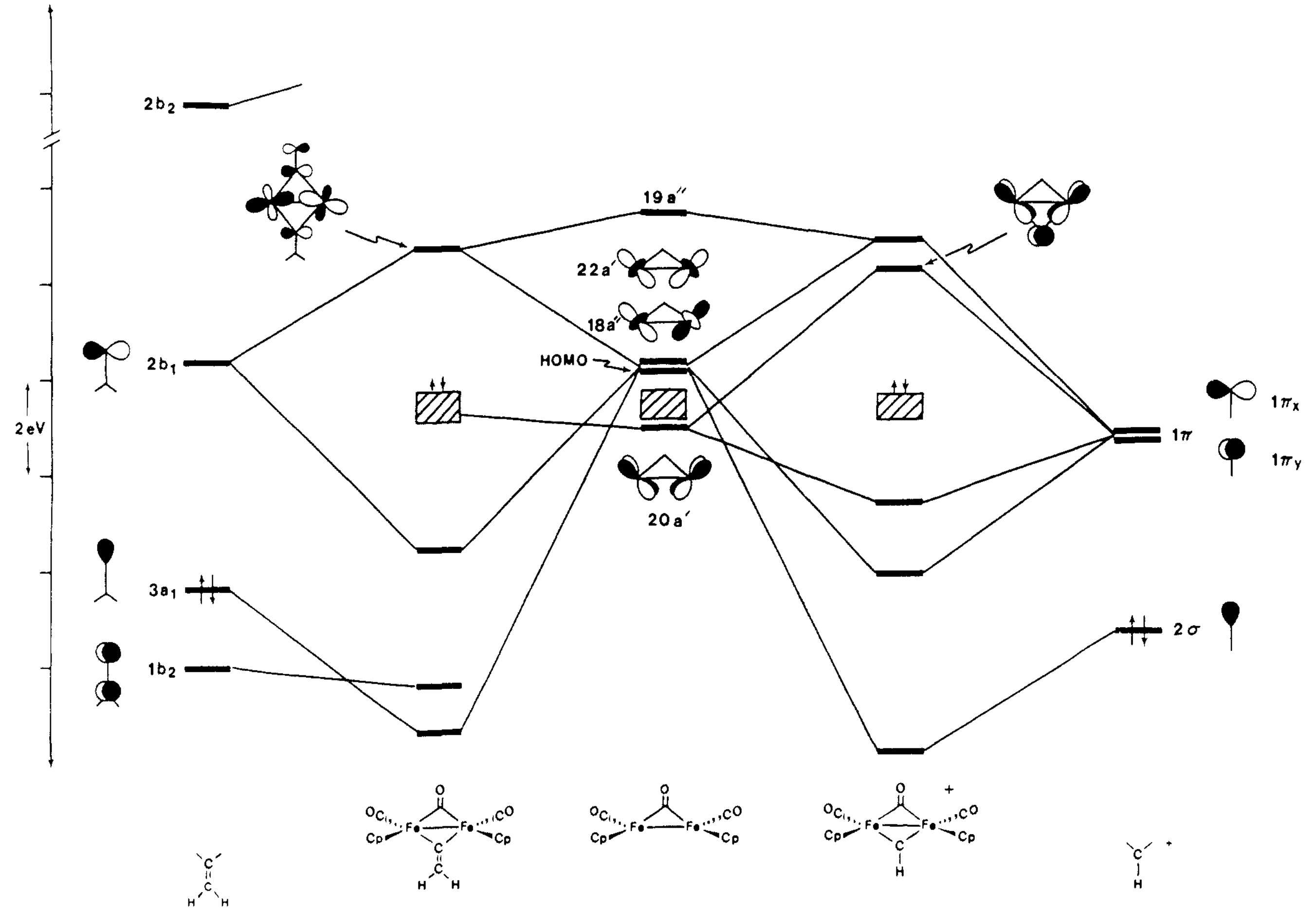

Figure 4. Molecular orbital diagrams of *cis*-[(η^5-C_5H_5)Fe(CO)]$_2$(μ-CO)(μ-C=CH_2) and *cis*-[(η^5-C_5H_5)Fe(CO)]$_2$(μ-CO)(μ-CH)$^+$.

however. Equally unclear is the nature of the precursor of the dimetallacyclic product 5C; it might be formed by prolonged photolysis of 5B, as shown in eq 5, or it may be formed directly from 5A under the assumption that the 5A–5B conversion is reversible, in a LUMO-controlled reaction similar to those discussed earlier. Thus we are somewhat reluctant to discuss the reactions in eq 5 in the absence of more detailed mechanistic studies. However, further support for the associative mechanism arises from the reactivity of the vinylidene bridge with diazoalkanes, a matter which we will now address.

As was pointed out earlier (Figure 4), the C–C π bond of the vinylidene remains localized on the ligand, essentially giving rise to a 1,1-dimetallated olefin. It is not surprising then that treatment with diazoalkanes in the presence of CuI causes addition across the double bond to produce 1,2-dimetallospiropentanes (eq 6),[37] in analogy with purely organic olefins. However, when the addition of diazoalkanes is carried out under photolytic conditions, an allene-bridged dimer results (eq 7).[37] It is this latter reaction which provides the most convincing evidence for the existence of intermediate IIB in Scheme II. If the primary photochemical step is indeed cleavage of the Fe–Fe bond and the Fe–(μ-C) bond, this would result in the formation of an Fe–C double bond in the proposed intermediate IIB. Thus, addition of the diazoalkane across this newly generated double bond or at the coordinatively unsaturated Fe atom would lead to the allene product (which may be formally thought of as a 1,4-dimetallaspiropentane). Precedent for carbene addition to a complex with just such a bridging ligand has been established by Knox and co-workers with an isovalent piano-stool dimer system of molybdenum (eq 8).[38]

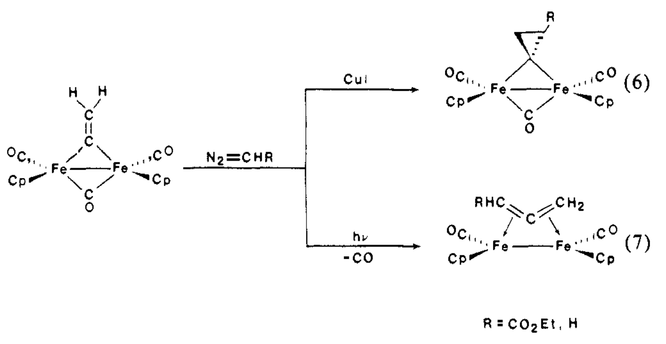

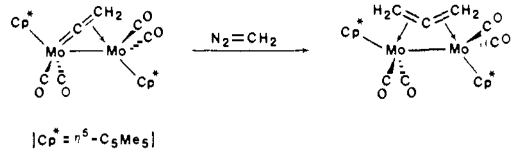

(8)

|Cp* = η^5-C_5Me_5|

Reactions at the Methylidyne Bridge. The chemistry of the methylidyne-bridged iron dimer is dominated by its reactivity with nucleophiles. Casey et al. have performed extensive studies on this system and have found the methylidyne bridge to very reactive even toward weak nucleophiles such as CO and alkenes (eq 9).[9b,c]

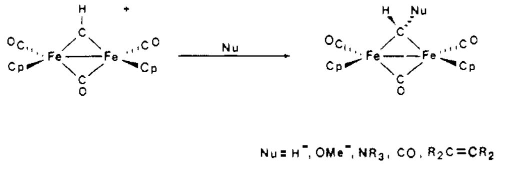

(9)

Nu = H$^-$, OMe$^-$, NR_3, CO, R_2C=CR_2

In each case the nucleophile adds directly to the bridging me-

---

[37] (a) Casey, C. P.; Austin, E. A. *Organometallics* **1986**, *5*, 584–585. (b) Hoel, E. L.; Ansell, G. B.; Leta, S. *Organometallics* **1986**, *5*, 585–587. (c) Hoel, E. L.; Ansell, G. B.; Leta, S. *Organometallics* **1984**, *3*, 1633–1637.

[38] Doherty, N. M.; Elschenbroich, C.; Kneuper, H.-J.; Knox, S. A. R. *J. Chem. Soc., Chem. Commun.* **1985**, 170–171.

thylidyne carbon (for Nu = $H_2C{=}CH_2$ a subsequent 1,2-hydrogen shift occurs to yield the "hydrocarbation" product). We believe this is a direct result of orbital controlled reactivity. The LUMO of this system was found to consist primarily of a $p\pi$ orbital on the μ-carbon of the methylidyne ligand (see Figure 4). This orbital is oriented perpendicular to the Fe–(μ-CH)–Fe plane and is sterically accessible. Nucleophiles can readily add to this relatively low-lying vacant orbital. Further evidence for either orbital-controlled or charge-controlled reactivity has been found in calculations on the isoelectronic $[\mathrm{CpFe(NO)}]_2(\mu\text{-CH})^+$[39] and $[\mathrm{CpRh(CO)}]_2(\mu\text{-CH}_2)$[40] systems which will be presented in a subsequent paper.

Conclusions

We have demonstrated that the Fenske–Hall molecular orbital method provides an accurate picture of the electronic structure of this series of organically bridged dimeric piano-stool complexes and can be particularly useful when applied to the understanding of their reactivity patterns. The method has also provided us a unique and promising approach into the mechanistic aspects of photochemical insertion of alkynes into various organic bridges. Although it is impossible to precisely model the entire reaction coordinate for a given reaction via molecular orbital calculations, we feel that particular electronic interactions of the reactants and/or products can be used to allow an understanding of certain preferred reactivity modes. It is also clear that more detailed studies, e.g., total energy calculations on potential surfaces involved in the photolysis mechanism as well as the wavelength dependence of the photochemistry of piano-stool dimers, are essential to test some of our conclusions.

We are expanding our studies to a wide variety of related piano-stool dimer systems (both homonuclear and heteronuclear) in order to assess the generality of this method for relating reactivity to electronic structure.

Acknowledgment. We would like to thank Professor Charles P. Casey for helpful discussions and critical comments. R.H.C. is grateful to The Ohio State University Graduate School for a Presidential Fellowship.

---

(39) (a) Casey, C. P.; Roddick, D. M. *Organometallics* **1986**, *5*, 436–438. (b) Cayton, R. H.; Bursten, B. E. *Abstracts of Papers*, 191st National Meeting of the American Chemical Society, New York, New York; Americal Chemical Society: Washington, DC, INOR 188.

(40) Herrmann, W. A.; Kruger, C.; Goddard, R.; Bernal, I. *J. Organomet. Chem.* **1977**, *140*, 73–89.

Probing the Design of a Novel Ditopic Anion Receptor

Franz P. Schmidtchen

Contribution from the Lehrstuhl für Organische Chemie und Biochemie der TU München, D-8046 Garching, FRG. Received June 20, 1986

Abstract: In an attempt to increase host–guest selectivity an open chain ditopic receptor **5** composed of two tetrahedral anion binding subunits which are connected by a *p*-xylene bridge was synthesized. The preparation produced the target host **5** in four steps in 23% yield starting from the macrotricyclic modules **4** and **6**. The selectivity advantage of the ditopic receptor design was investigated by using the dimensional probes **10–14**. Association constants of the probes with the ditopic **5** or monotopic **2** were calculated from a Benesi–Hildebrand treatment of the optical effects occurring on host–guest complexation. The comparison of selectivity ratios derived therefrom reveals a sharp increase with **13** and **14** demonstrating the participation of both receptor subunits of **5** in binding these guests. The superiority of the ditopic vs. a monotopic receptor design amounts to a factor of 3. The *p*-xylene connecting unit is sufficiently rigid to define a minimum distance of approach of the two subunits of the ditopic host **5**.

How can selectivity be introduced into chemical reactions? One possibility to approach this fundamental problem[1,2] is to force the reaction partners into spatial and temporal proximity in their ground states prior to any chemical conversion event.[3] This principle is ubiquitous in the living world naming enzymic catalysis, membrane transport, hormonal signal transduction, replication, metabolic regulation, and friend–foe recognition in the immune response as a few shining examples. There is no equivalent in abiotic chemistry at present though the fascinating perspectives of the approach are generally recognized.[4-6] Prerequisite to the rational application of this principle in artificial systems is the availability of host molecules capable of recognizing and specifically binding the reaction partners from a variety of structurally related species. The recognition process may, for instance, exclusively respond to the shape and the molecular dimensions of the guests. Corresponding hosts can be tailored by using synthetic polymers,[7,8] but inorganic analogues (e.g., zeolites) owing their ability to discriminate potential guests by shape to a peculiar crystal structure have already found widespread use in industrial chemistry.[9,10] It is intuitively comprehensible that the guest specificity of these hosts will be optimized the more extensive and precise the surface of the guest can be scanned. Rigid and geo-

---

(1) (a) Trost, B. M. *Chem.* (*Britain*) **1984**, *20*, 315. (b) *Selectivity—A Goal for Synthetic Efficiency*; Bartmann, W., Trost, B. M., Eds.; Verlag Chemie: Weinheim, 1984.

(2) (a) Breslow, R. *Science* (Washington, DC) **1982**, *218*, 532. (b) Breslow, R. *Acc. Chem. Res.* **1980**, *13*, 170.

(3) (a) Menger, F. M. *Acc. Chem. Res.* **1985**, *18*, 128. (b) Menger, F. M.; Venkataram, U. V. *J. Am. Chem. Soc.* **1985**, *107*, 4706.

(4) Lehn, J.-M. *Science* (*Washington, DC*) **1985**, *227*, 849.

(5) See, e.g., recent reviews on enzyme models and general host-guest chemistry: (a) Tabushi, I. *Tetrahedron* **1984**, *40*, 269. (b) Murakami, Y. *Top. Curr. Chem.* **1983**, *115*, 107. (c) Sirlin, C. *Bull. Soc. Chim. Fr.* **1984**, *2*, 5. (d) Purmal, A. P.; Nikolaev, L. A. *Russ. Chem. Rev.* **1985**, *54*, 466. (e) Schmidtchen, F. P. *Top. Curr. Chem.* **1986**, *132*, 101. (f) *Host-Guest Complex Chemistry/Macrocycles*; Vögtle, F., Weber, E., Eds.; Springer: Berlin, 1985.

(6) (a) D'Sousa, V. T.; Hanabusa, K.; O'Leary, T.; Gadwood, R. C.; Bender, M. L. *Biochem. Biophys. Res. Commun.* **1985**, *129*, 727. (b) Menger, F. M.; Whitesell, L. G. *J. Am.* Chem. *Soc.* **1985**, *107*, 707. (c) Cram, D. J.; Yuk-Sun Lam, P.; Ho, S. P. *J. Am. Chem. Soc.* **1986**, *108*, 839. (d) Breslow, R.; Czarnik, A. W.; Lauer, M.; Leppkes, R.; Winkler, J.; Zimmerman, S. *J. Am. Chem. Soc.* **1986**, *108*, 1969.

(7) Wulff, G.; Heide, B.; Helfmeier, G. *J. Am. Chem. Soc.* **1986**, *108*, 1089.

(8) Shea, K. J.; Dougherty, T. K. *J. Am. Chem. Soc.* **1986**, *108*, 1091.

(9) Vedrine, J. C. *ACS Symp. Ser.* **1985**, *279*, 257.

(10) Csicsery, S. M. *Pure Appl. Chem.* **1986**, *58*, 841.

0002-7863/86/1508-8249$01.50/0 © 1986 American Chemical Society